



Scholars Research Library

Der Pharma Chemica, 2014, 6(5):220-234
(<http://derpharmachemica.com/archive.html>)



ISSN 0975-413X
CODEN (USA): PCHHAX

Combined electrochemical and quantum chemical study of new quinoxaline derivative as corrosion inhibitor for carbon steel in acidic media

H. Tayebi¹, H. Bourazmi¹, B. Himmi⁴, A. El Assyry⁵, Y. Ramli³, A. Zarrouk², A. Geunbour¹ and B. Hammouti²

¹Laboratoire Corrosion-Électrochimie, Faculté des Sciences, Université Mohamed V, Rabat, Morocco

²LCAE-URAC18, Faculté des Sciences, Université Mohammed I^{er}, Oujda, Morocco

³Laboratoire de Chimie Thérapeutique, Faculté de Médecine et de Pharmacie de rabat, Université Mohamed V, Rabat, Morocco

⁴Filière Techniques de Santé, Institut des Professions Infirmières et des Techniques de Santé de Rabat, Morocco

⁵Laboratoire d'Optoélectronique et de Physico-chimie des Matériaux (Unité associée au CNRST), Département de Physique, Université Ibn Tofail, Kénitra, Maroc

ABSTRACT

2-(8-hydroxyquinoxalin-5-yl)acetonitrile (QIN3) was tested as corrosion inhibitor for carbon steel in 1.0 M HCl by using polarization and electrochemical impedance spectroscopy (EIS) at 303-333K. The inhibition efficiency was found to increase with increase in QIN3 concentration but decreased with temperature. Activation parameters and Gibbs free energy for the adsorption process were calculated and discussed. Potentiodynamic polarization curves indicated that the quinoxaline derivative as mixed-type inhibitor. Impedance measurements showed that the double-layer capacitance decreased and charge-transfer resistance increased with increase in the inhibitor concentration and hence increasing in inhibition efficiency. The quantum chemical calculations were performed at the density functional theory (DFT) level using B3LYP functional with the 6-31G (d).

Keywords: Steel, HCl, Corrosion inhibition, Electrochemical techniques, DFT.

INTRODUCTION

The use of inhibitors is one of the most practical methods for protection of metal against corrosion, especially in acidic media [1]. Most of the well-known acid inhibitors are organic compounds containing nitrogen, sulphur, and oxygen atoms. Compounds with π -electrons and functional groups containing heteroatoms which can donate lone pair electrons are found to be particularly useful as inhibitors for corrosion of metals [2-31]. The exiting data reveal that most organic inhibitors act by adsorption on the metal surface. This adsorption is influenced by the nature and surface charge of metal, the type of aggressive electrolyte and the chemical structure of inhibitors [32]. The inhibiting actions of organic compounds are usually attributed to their interactions with the metal surface through adsorption. The adsorption of these compounds onto the metal surface depends on the nature and surface charge of the metal, the chemical composition of electrolytes, and the molecular structure and electronic characteristics of the inhibitor molecules.

Recently, various experimental and theoretical techniques have been developed to study the structural properties of inhibitor molecules and their activity toward metal surface, but the quantum chemical calculations based on density function theory (DFT) method have become an attractive theoretical method because it gives exact basic vital parameters for even huge complex molecules. Thus, DFT has become an important tool for connecting some traditional empirical concepts with quantum mechanics [33]. Therefore, DFT is a very powerful technique to probe inhibitor/surface interaction and to analyze experimental data.

The aim of the present work was to investigate the effects of 2-(8-hydroxyquinoxalin-5-yl)acetonitrile as inhibitor for the corrosion of carbon steel in 1.0 M HCl solutions. Potentiodynamic polarization and electrochemical impedance spectroscopy (EIS) measurements were employed to evaluate the corrosion rate of carbon steel and the inhibition efficiencies of this compound. The relationships between the inhibition efficiency of the used compound in 1.0 M HCl and some quantum chemical parameters such as E_{HOMO} (highest occupied molecular orbital energy), E_{LUMO} (lowest unoccupied molecular orbital energy), the energy gap (ΔE), hardness(η), Softness(S), dipole moment(μ), electron affinity(EA), ionization potential(IE), the absolute electronegativity (χ), electrophilicity index(ω) and the fraction of electron transferred (ΔN) have been also investigated by quantum chemical calculations. The selected organic compound which still has not been studied contains nitrogen and oxygen atoms and two aromatic rings. The molecular structure of 2-(8-hydroxyquinoxalin-5-yl)acetonitrile (QIN3) is given in Fig. 1.

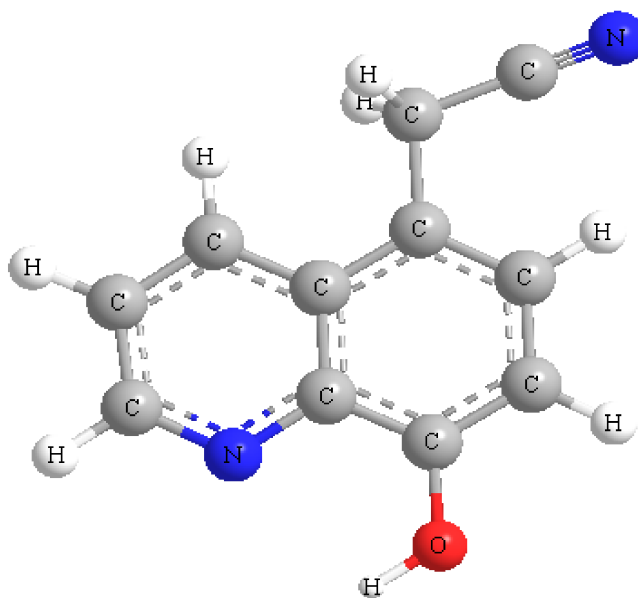


Fig. 1 Chemical structure of 2-(8-hydroxyquinoxalin-5-yl)acetonitrile (QIN3)

MATERIALS AND METHODS

Materials

The steel used in this study is a carbon steel (CS) (Euronorm: C35E carbon steel and US specification: SAE 1035) with a chemical composition (in wt%) of 0.370 % C, 0.230 % Si, 0.680 % Mn, 0.016 % S, 0.077 % Cr, 0.011 % Ti, 0.059 % Ni, 0.009 % Co, 0.160 % Cu and the remainder iron (Fe).

Solutions

The aggressive solutions of 1.0 M HCl were prepared by dilution of analytical grade 37% HCl with distilled water. The concentration range of 2-(8-hydroxyquinoxalin-5-yl)acetonitrile (QIN3) used was 10^{-6} M to 10^{-3} M.

Polarization measurements

Electrochemical impedance spectroscopy

The electrochemical measurements were carried out using Volta lab (Tacussel- Radiometer PGZ 100) potentiostat and controlled by Tacussel corrosion analysis software model (Voltmaster 4) at under static condition. The corrosion cell used had three electrodes. The reference electrode was a saturated calomel electrode (SCE). A platinum electrode was used as auxiliary electrode of surface area of 1 cm^2 . The working electrode was carbon steel. All potentials given in this study were referred to this reference electrode. The working electrode was immersed in test solution for 30 minutes to establish steady state open circuit potential (E_{ocp}). After measuring the E_{ocp} , the electrochemical measurements were performed. All electrochemical tests have been performed in aerated solutions at 303 K. The EIS experiments were conducted in the frequency range with high limit of 100 kHz and different low limit

0.1 Hz at open circuit potential, with 10 points per decade, at the rest potential, after 30 min of acid immersion, by applying 10 mV ac voltage peak-to-peak. Nyquist plots were made from these experiments. The best semicircle can be fit through the data points in the Nyquist plot using a non-linear least square fit so as to give the intersections with the x -axis.

The inhibition efficiency of the inhibitor was calculated from the charge transfer resistance values using the following equation [34]:

$$\eta_z \% = \frac{R_{ct}^i - R_{ct}^\circ}{R_{ct}^i} \times 100 \quad (1)$$

where, R_{ct}° and R_{ct}^i are the charge transfer resistance in absence and in presence of inhibitor, respectively.

Potentiodynamic polarization

The electrochemical behaviour of carbon steel sample in inhibited and uninhibited solution was studied by recording anodic and cathodic potentiodynamic polarization curves. Measurements were performed in the 1.0 M HCl solution containing different concentrations of the tested inhibitor by changing the electrode potential automatically from -800 to 0 mV versus corrosion potential at a scan rate of 1 mV s⁻¹. The linear Tafel segments of anodic and cathodic curves were extrapolated to corrosion potential to obtain corrosion current densities (I_{corr}). From the polarization curves obtained, the corrosion current (I_{corr}) was calculated by curve fitting using the equation:

$$I = I_{corr} \left[\exp\left(\frac{2.3\Delta E}{\beta_a}\right) - \exp\left(\frac{2.3\Delta E}{\beta_c}\right) \right] \quad (2)$$

The inhibition efficiency was evaluated from the measured I_{corr} values using the relationship:

$$\eta_{Tafel} \% = \frac{I_{corr}^\circ - I_{corr}^i}{I_{corr}^\circ} \times 100 \quad (3)$$

where, I_{corr}° and I_{corr}^i are the corrosion current density in absence and presence of inhibitor, respectively.

Quantum chemical calculations

Complete geometrical optimizations of the investigated molecules are performed using DFT (density functional theory) with the Beck's three parameter exchange functional along with the Lee-Yang-Parr nonlocal correlation functional (B3LYP) [35-37] with 6-31G* basis set is implemented in Gaussian 03 program package [38]. This approach is shown to yield favorable geometries for a wide variety of systems. This basis set gives good geometry optimizations. The geometry structure was optimized under no constraint. The following quantum chemical parameters were calculated from the obtained optimized structure: The highest occupied molecular orbital (E_{HOMO}) and the lowest unoccupied molecular orbital (E_{LUMO}), the energy difference (ΔE) between E_{HOMO} and E_{LUMO} , dipole moment (μ), electron affinity (A), ionization potential (I) and the fraction of electrons transferred (ΔN).

RESULTS AND DISCUSSION

Potentiodynamic polarization

Figure 2 showed potentiodynamic polarization curves for the carbon steel electrode in 1.0 M HCl solution with and without different concentrations of QIN3. It is clear that the current density decreases with the presence of quinoxaline derivative; this indicated that QIN3 adsorbed on the metal surface, and hence inhibition occurs. Values of corrosion potential (E_{corr}) and corrosion current density (I_{corr}), obtained by extrapolation of the Tafel lines, cathodic Tafel slope (β_c), and η_{Tafel} (%) for different concentrations of QIN3 in 1.0 M HCl, are given in Table 1. The potentiodynamic curves show that there is a clear reduction of both the anodic and cathodic currents in the presence of QIN3 compared with those for the blank solution.

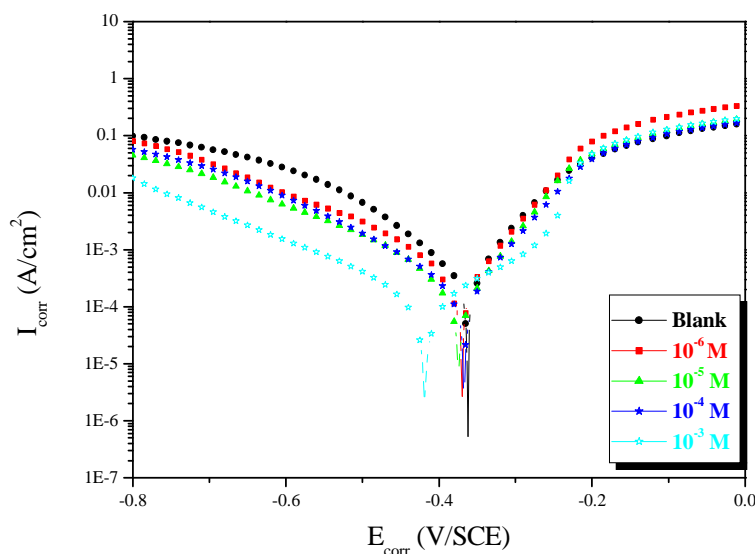


Figure 2. Polarization curves for the corrosion of carbon steel in 1.0 M HCl with different concentrations of QIN3 at 303 K

Table 1. Potentiodynamic electrochemical parameters for the corrosion of carbon steel in 1.0 M HCl solution in the absence and presence of the investigated inhibitor at 303 K

Inhibitor	Conc (M)	$-E_{\text{corr}}$ (mV _{SCE})	$-\beta_c$ (mV/dec)	I_{corr} ($\mu\text{A cm}^{-2}$)	η_{Tafel} (%)
Blank	1.0	362	123.8	335	-----
QIN3	10^{-3}	419	159.8	17.2	95
	10^{-4}	368	131.8	59.5	82
	10^{-5}	374	133.4	62.9	81
	10^{-6}	369	121.3	66.9	80

It is clear from the electrochemical polarisation results that the addition of inhibitor causes a decrease of the current density. The values I_{corr} of carbon steel in the inhibited solution are smaller than those for the inhibitor free solution (Table 1). The parallel cathodic Tafel plots obtained in Fig. 2 indicate that the hydrogen evolution is activation-controlled and the reduction mechanism is not affected by the presence of inhibitor. The anodic branches are slightly affected in the presence of this inhibitor. However, a shift of corrosion potential (E_{corr}) towards cathodic side i.e -362 to -419 mV was established. In literature, [39] it has been reported that (i) if the displacement in E_{corr} is >85 mV with respect to E_{corr} , the inhibitor can be seen as a cathodic or anodic type and (ii) if displacement in E_{corr} is <85 , the inhibitor can be seen as mixed type. In the present study, shift in E_{corr} values is in the range of 6-57 mV, so we can classify our inhibitor as mixed inhibitor with predominant cathodic effectiveness. Adsorption is the mechanism that is generally accepted to explain the inhibitory action of organic corrosion inhibitors. The adsorption of inhibitors can affect the corrosion rate in two ways: (i) by decreasing the available reaction area, i.e., the so-called geometric blocking effect, and (ii) by modifying the activation energy of the cathodic and/or anodic reactions occurring in the inhibitor-free metal in the course of the inhibited corrosion process. It is a difficult task to determine which aspects of the inhibiting effect are connected to the geometric blocking action and which are connected to the energy effect.

Electrochemical Impedance Spectroscopy Measurements

Effect of concentration

The experimental results obtained from EIS measurements for the corrosion of carbon steel in the presence of quinoxaline derivative at 303K are summarized in Table 2. The impedance spectra for carbon steel in 1.0 M HCl solution without and with different concentration of QIN3 are presented as Nyquist plots in Fig. 3. Clearly, the impedance spectra exhibit a large capacitive loop at high frequencies. The capacitive loop indicates that the corrosion of steel is mainly controlled by a charge transfer process, and usually related to the charge transfer of the corrosion process and double-layer behavior. The diameter of the capacitive loop in the presence of the inhibitor is larger than in the absence of the inhibitor (blank solution) and increases with the inhibitor concentration. This indicates that the impedance of inhibited substrate increases with the inhibitor concentration. Noticeably, these capacitive loops are not perfect semicircles which can be attributed to the frequency dispersion effect. This anomalous behavior is generally attributed to the roughness and inhomogeneity of the metal surface [40].

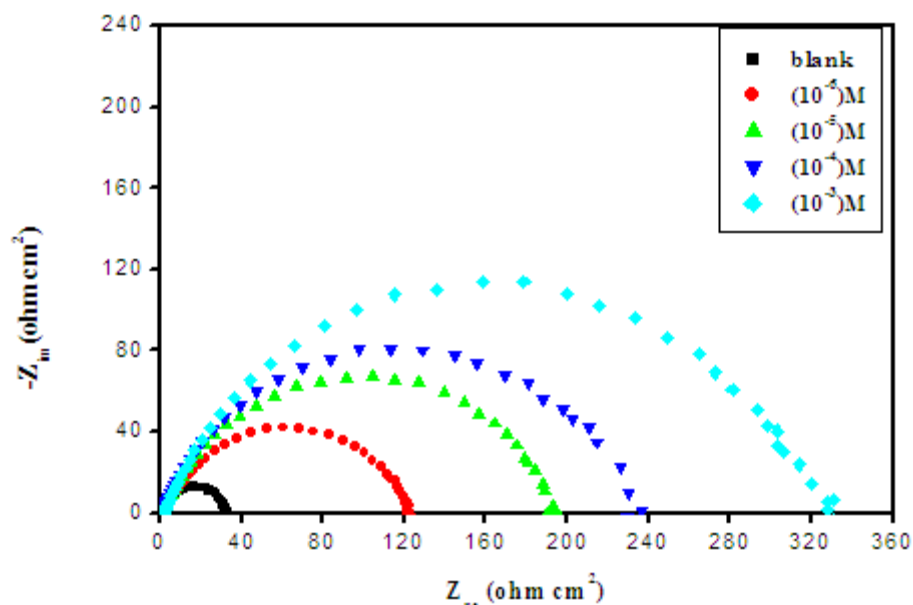


Figure 3. Nyquist plots of carbon steel in 1.0 M HCl with various concentrations of QIN3

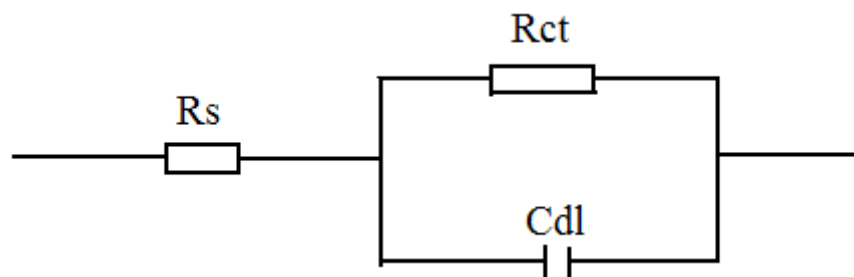


Figure 4. Randles electrical equivalent circuit (R_s solution resistance, R_{ct} charge transfer resistance, C_{dl} double-layer capacitance)

The simplest fitting is represented by Randles electrical equivalent circuit in Fig. 4, which is a parallel combination of the charge transfer resistance R_{ct} and the constant phase element, CPE_{dl} , both in series with the solution resistance (R_s) [41]. It can be seen that addition of the inhibitor increases the values of charge transfer resistance (R_{ct}) and reduces the double-layer capacitance (C_{dl}). The interfacial double-layer capacitance (C_{dl}) values have been estimated from the impedance value using Nyquist plot by the formula:

$$C_{dl} = (2\pi f_{max} R_{ct})^{-1} \quad (4)$$

The values of C_{dl} decreased with an increase in the inhibitor concentration. This was due to an increase in the surface coverage by this inhibitor, resulting into an increase in the inhibition efficiency. The thickness of the productive layer, δ_{inh} was related to C_{dl} by the following equation [42],

$$\delta_{inh} = \frac{\epsilon_0 \epsilon_r}{C_{dl}} \quad (5)$$

where ϵ_0 is the dielectric constant and ϵ_r is the relative dielectric constant. This decrease in C_{dl} values from 128 to 24 $\mu F cm^{-2}$ is due to the reduction in the local dielectric constant and/or an increment in the thickness of the electrical double layer. The phenomenon proposed that the inhibitor molecules function by adsorption at the metal/solution interface. Thus, the change in C_{dl} is due to the gradual replacement of the water molecules by the adsorption of the inhibitor molecules on the metal surface, decreasing the magnitude of metal dissolution [43]. The increase in R_{ct} values from 31 to 331 Ωcm^2 is due to the formation of a productive film on the metal/solution interface [44]. These observations suggest that quinoxaline molecules function by adsorption at the metal surface, thus causing the decrease in C_{dl} values and increase in R_{ct} values. Table 2 confirms that the inhibition efficiency ($\eta_z\%$) increases with

the concentrations of QIN3, and that the maximum efficiency (91) reaches 1.0 mM of inhibitor. All the above results infer that, with increases in quinoxaline derivative concentration, the productive film is more and more protective.

Table 2. Electrochemical impedance parameters for carbon steel in 1.0 M HCl containing different concentrations of QIN3

	Conc (M)	R_{ct} ($\Omega \text{ cm}^2$)	C_{dl} ($\mu\text{F}/\text{cm}^2$)	f_{max} (Hz)	η_z (%)	θ
Blank	1.0	31	128	40.0	---	-----
QIN3	10^{-3}	331	24	20.0	91	0.91
	10^{-4}	263	48	12.5	88	0.88
	10^{-5}	163	52	15.8	84	0.84
	10^{-6}	122	104	12.5	75	0.75

Effect of temperature

The effect of temperature on the inhibition efficiencies of QIN3 was also studied by EIS in the temperature range 303-333K (Figs. 5 and 6). The various corrosion parameters obtained are listed in Table 3. The data obtained suggest that QIN3 get adsorbed on the steel surface at all temperatures studied. Inspection of Table 3 showed that, the temperature rise leads to a decrease of R_{ct} values. This is due on one hand to the increase of the rate of metal dissolution, while on the other hand to the shift of the adsorption/desorption equilibrium towards the inhibitor's desorption and hence to the decrease of surface coverage degree.

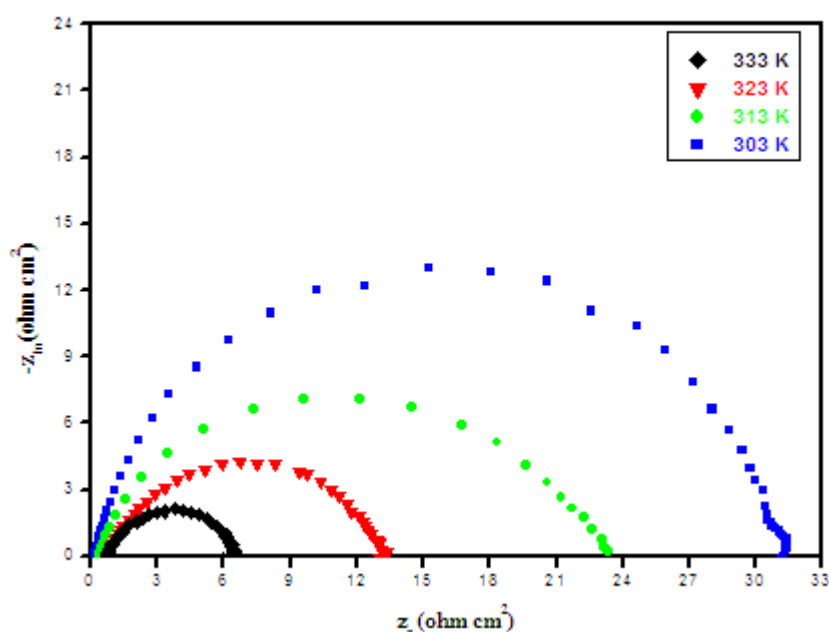


Figure 5. Nyquist diagrams for carbon steel in 1.0 M HCl at different temperatures

Table 3. EIS parameters and the corresponding inhibition efficiencies at various temperatures studied of carbon steel in 1.0 M HCl containing different concentrations of QIN3.

Inhibitor	Temp (K)	R_{ct} ($\Omega \text{ cm}^2$)	f_{max} (Hz)	C_{dl} ($\mu\text{F}/\text{cm}^2$)	η_z (%)
Blank	303	31	128	40	---
	313	27	40	147	---
	323	12	79	163	---
	333	6	158	168	---
QIN3	303	333	20	24	91
	313	284	12.5	45	90
	323	59	40	67	80
	333	23	79	88	73

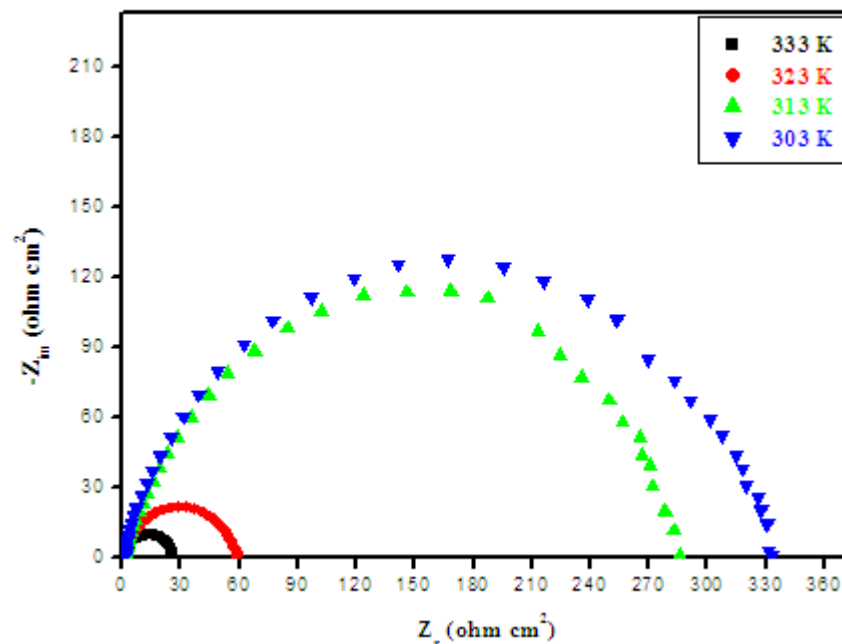


Figure 6. Nyquist diagrams for carbon steel in 1.0 M HCl + 10^{-3} M of QIN3 at different temperatures

Values of R_{ct} were employed to calculate values of the corrosion current density (I_{corr}) at various temperatures in absence and presence of CTPTC using the following equation [45]:

$$I_{corr} = RT(zFR_{ct})^{-1} \quad (6)$$

where R is the universal gas constant ($R = 8.314 \text{ J mol}^{-1} \text{ K}^{-1}$), T is the absolute temperature, z is the valence of iron ($z = 2$), F is the Faraday constant ($F = 96485 \text{ coulomb}$) and R_{ct} is the charge transfer resistance.

The activation parameters for the corrosion reaction can be regarded as an Arrhenius-type process, according to the following equation:

$$I_{corr} = A \exp\left(-\frac{E_a}{RT}\right) \quad (7)$$

where E_a is the apparent activation corrosion energy, R is the universal gas constant, and A is the Arrhenius preexponential factor. The apparent activation energies (E_a) in the absence and in the presence of various concentrations of QIN3 are calculated by linear regression between $\ln(I_{corr})$ and $1/T$ (Figure 7), and the results are given in Table 4. All the linear regression coefficients are close to 1, indicating that the steel corrosion in hydrochloric acid can be elucidated using the kinetic model. As observed from Table 4, the E_a increased with increasing concentration of QIN3, but all values of E_a in the range of the studied concentration were higher than that of the uninhibited solution. The increase in E_a in the presence of QIN3 may be interpreted as physical adsorption. Indeed, a higher energy barrier for the corrosion process in the inhibited solution is associated with physical adsorption or weak chemical bonding between the inhibitor species and the steel surface [46, 47]. Szauer and Brand. explained that the increase in activation energy can be attributed to an appreciable decrease in the adsorption of the inhibitor on the carbon steel surface with the increase in temperature. A corresponding increase in the corrosion rate occurs because of the greater area of metal that is consequently exposed to the acid environment [48].

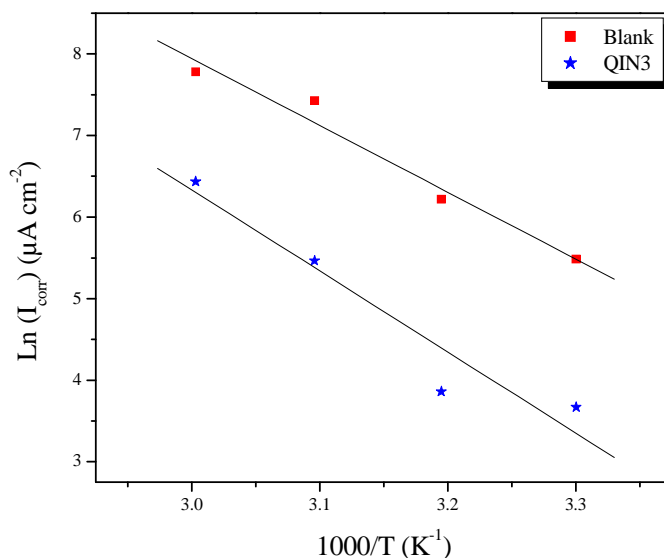


Figure 7. Arrhenius plots for carbon steel corrosion rates $\text{Ln}(I_{\text{corr}})$ versus $1/T$ in 1.0 M HCl in absence and in presence of optimum concentration of QIN3

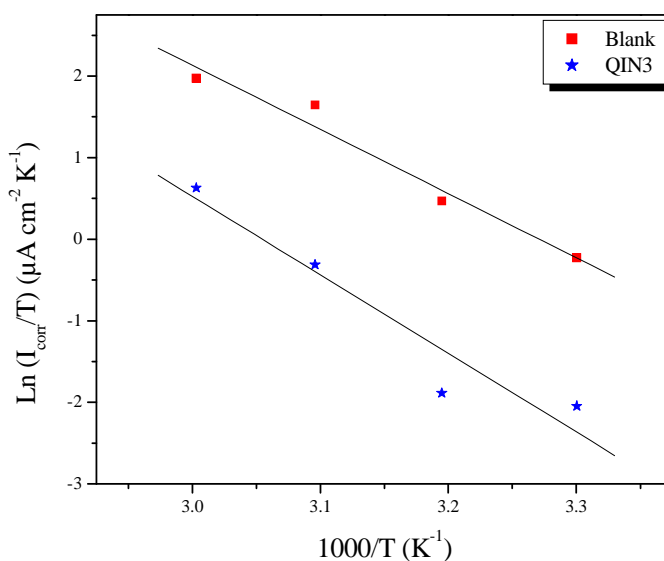


Figure 8. Transition-state plots for carbon steel corrosion rates $\text{Ln}(I_{\text{corr}}/T)$ versus $1/T$ in 1.0 M HCl in absence and in presence of optimum concentrations of QIN3

Table 4. The value of activation parameters for carbon steel in 1.0 M HCl in the absence and presence of optimum concentration of QIN3

	E_a (kJ mol ⁻¹)	ΔH_a (kJ mol ⁻¹)	ΔS_a (J mol ⁻¹ K ⁻¹)
Blank	68.03	65.39	16.37
QIN3	82.61	82.47	46.74

The enthalpy of activation (ΔH_a) and the entropy of activation (ΔS_a) for the intermediate complex in the transition state for the corrosion of carbon steel in 1.0 M HCl in the absence and in the presence of optimum concentration QIN3 were obtained by applying the alternative formulation of Arrhenius equation [49]:

$$I_{corr} = \frac{RT}{Nh} \exp\left(\frac{\Delta S_a}{R}\right) \exp\left(\frac{\Delta H_a}{RT}\right) \quad (8)$$

where h is the Plank's constant and N is the Avogadro's number. Figure 8 shows a plot of $\ln(I_{corr}/T)$ versus $1/T$. A straight lines are obtained with a slope of $(-\Delta H_a/R)$ and an intercept of $(\ln R/Nh + \Delta S_a/R)$ from which the values of ΔH_a and ΔS_a were calculated (Table 4). The positive values of ΔH_a in the absence and the presence of QIN3 reflect the endothermic nature of the carbon steel dissolution process.

In addition, the value of ΔS_a were higher for inhibited solutions than that for the uninhibited solution (Table 4). This suggested that an increase in randomness occurred on going from reactants to the activated complex. This might be the results of the adsorption of organic inhibitor molecules from the nitric solution could be regarded as a quasi-substitution process between the organic compound in the aqueous phase and water molecules at electrode surface [50]. In this situation, the adsorption of organic inhibitor was accompanied by desorption of water molecules from the surface. Thus the increasing in entropy of activation was attributed to the increasing in solvent entropy [51].

Adsorption Isotherm.

The adsorption on the corroding surfaces never reaches the real equilibrium and tends to reach an adsorption steady state. However, when the corrosion rate is sufficiently small, the adsorption steady state has a tendency to become a quasi-equilibrium state. In this case, it is reasonable to consider the quasi-equilibrium adsorption in a thermodynamic way using the appropriate equilibrium isotherms [52]. The efficiency of the quinoxaline derivative as a successful corrosion inhibitor mainly depends on its adsorption ability on the metal surface. So, it is essential to know the mode of adsorption and the adsorption isotherm that can give valuable information on the interaction of inhibitor and metal surface. The surface coverage values, θ ($\theta = (\eta_z / \%) / 100$), for different concentrations of QIN3 were used to explain the best adsorption isotherm. A plot of C_{inh}/θ versus C_{inh} (Figure 9) gives a straight line with an average correlation coefficient of 1 and a slope of nearly unity suggests that the adsorption of QIN3 molecules obeys Langmuir adsorption isotherm, which can be expressed by the following equation:

$$\frac{C_{inh}}{\theta} = \frac{1}{K_{ads}} + C_{inh} \quad (9)$$

where C_{inh} is the inhibitor concentration, K_{ads} is the adsorption equilibrium constant and θ is the surface coverage.

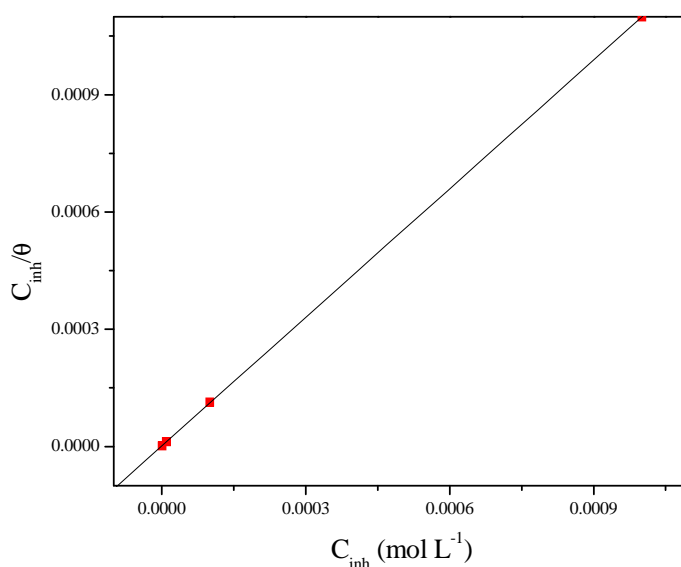


Figure 9. Langmuir's isotherm adsorption model of QIN3 on the carbon steel surface in 1.0 M HCl

From the intercepts of the straight lines on the C_{inh}/θ -axis (Figure 9), K_{ads} can be calculated which is related to free energy of adsorption, ΔG_{ads}° as given by:

$$\Delta G_{ads}^{\circ} = -RTL \ln(55.5K_{ads}) \quad (10)$$

The negative value of ΔG_{ads}° ensure the spontaneity of the adsorption process and stability of the adsorbed film on the carbon steel surface [53]. It is usually accepted that the value of ΔG_{ads}° around -20 kJ mol^{-1} or lower indicates the electrostatic interaction between charged metal surface and charged organic molecules in the bulk of the solution while those around -40 kJ mol^{-1} or higher involve charge sharing or charge transfer between the metal surface and organic molecules [27].

The value of ΔG_{ads}° is equal to $-43.72 \text{ kJ mol}^{-1}$. The large value of ΔG_{ads}° and its negative sign is usually characteristic of strong interaction and a highly efficient adsorption [54]. The high value of ΔG_{ads}° shows that in the presence of 1.0 M HCl chemisorption of QIN3 may occur. The possible mechanisms for chemisorption can be attributed to the donation of π -electron in the aromatic rings, the presence of one oxygen and two nitrogen atoms in inhibitor molecule as reactive centers is an electrostatic adsorption of the protonated quinoxaline compound in acidic solution to adsorb on the metal surface.

Quantum Chemical Calculations

Recently, density functional theory (DFT) has been used to analyze the characteristics of the inhibitor/surface mechanism and to describe the structural nature of the inhibitor in the corrosion process. Furthermore, DFT is considered a very useful technique to probe the inhibitor/surface interaction as well as to analyze the experimental data. This technique has been found to be successful in providing insights into the chemical reactivity and selectivity in terms of global parameters such as electronegativity (χ), hardness (η), softness(S)... [55,56]. The basic relationship of the density functional theory of chemical reactivity is precisely, the one established by Parr, Donnelly, Levy and Palke [57], that links the chemical potential of DFT with the first derivative of the energy with respect to the number of electrons, and therefore with the negative of the electronegativity χ .

$$\mu = \left(\frac{\partial E}{\partial N} \right)_{v(r)} = -\chi \quad (11)$$

Where μ is the chemical potential, E is the total energy, N is the number of electrons, and $v(r)$ is the external potential of the system.

Hardness (η) has been defined within the DFT as $v(r)$ the second derivative of the E with respect to N as property which measures both the stability and reactivity of the molecule [58].

$$\eta = \left(\frac{\partial^2 E}{\partial N^2} \right)_{v(r)} \quad (12)$$

Where, $v(r)$ and μ are, respectively, the external and electronic chemical potentials.

According to, the Koopmans' theorem [59] for closed-shell molecules, ionization potential (I) and electron affinity (A) can be expressed as follows in terms of E_{HOMO} , E_{LUMO} the highest occupied molecular orbital energy, and the lowest unoccupied molecular orbital energy, respectively:

$$I = -E_{HOMO} \quad (13)$$

$$A = -E_{LUMO} \quad (14)$$

When the values of I and A are known, one can determine through the following expressions [60] the values of the absolute electronegativity χ , the absolute hardness η and the softness S (the inverse of the hardness):

$$\chi = \frac{I + A}{2} \quad (15)$$

$$\eta = \frac{I - A}{2} \quad (16)$$

The global softness(S) is the inverse of the global hardness [61]

$$S = \frac{1}{\eta} \quad (17)$$

For a reaction of two systems with different electronegativities the electronic flow will occur from the molecule with the lower electronegativity (the organic inhibitor) towards that of higher value (metallic surface), until the chemical potentials are equal [62]. Therefore the fraction of electrons transferred (ΔN) from the inhibitor molecule to the metallic atom was calculated according to Pearson electronegativity scale [63]

$$\Delta N = \frac{\chi_{Fe} - \chi_{inh}}{2(\eta_{Fe} + \eta_{inh})} \quad (18)$$

Where χ_{Fe} and χ_{inh} denote the absolute electronegativity of iron and inhibitor molecule respectively η_{Fe} and η_{inh} denote the absolute hardness of iron and the inhibitor molecule respectively. In this study, we use the theoretical value of $\chi_{Fe} = 7.0$ eV [64] and $\eta_{Fe} = 0$ eV by assuming that for a metallic bulk $I = A$ [65] because they are softer than the neutral metallic atoms. The difference in electronegativity drives the electron transfer, and the sum of the hardness parameters acts as a resistance [66].

Frontier orbital theory was useful in predicting the adsorption centers of the inhibitor molecule QIN3 responsible for its interaction with surface metal atoms [67]. Terms involving the frontier molecular orbital could provide a dominative contribution because of the inverse dependence of stabilization energy on orbital energy difference. Excellent corrosion inhibitors are usually organic compounds that not only offer electrons to unoccupied orbitals of the metal but also accept free electrons from the metal [68]. A relationship between the corrosion inhibition efficiency of the synthesized compound with the orbital energies of the HOMO (E_{HOMO}) and LUMO (E_{LUMO}) as well as the dipole moment (μ) are shown in Table 4. As is clearly observed in the Table 5, the inhibition efficiency increases with an increase in E_{HOMO} values along with a decrease in E_{LUMO} values.

The E_{HOMO} is often associated with the electron donating ability of a molecule. Therefore, increasing values of E_{HOMO} indicate a higher tendency for the donation of electron(s) to the appropriate acceptor molecule with low energy and an empty molecular orbital. Increasing values of E_{HOMO} thus facilitate the adsorption of the inhibitor. Consequently, improving the transport process through the adsorbed layer would enhance the inhibition efficiency of the inhibitor. This finding can be explained as follows. E_{LUMO} indicates the ability of the molecule to accept electrons; therefore, a lower value of E_{LUMO} more clearly indicates that the molecule would accept electrons [69]. The dipole moment (μ) is an index that can also be used to predict the direction of a corrosion inhibition process. Dipole moment is the measure of polarity in a bond and is related to the distribution of electrons in a molecule. Although literature is inconsistent on the use of μ as a predictor of the direction of a corrosion inhibition reaction, it is generally agreed that the adsorption of polar compounds possessing high dipole moments on the metal surface should lead to better inhibition efficiency. The data obtained from the present study indicate that the QIN3 inhibitor has the value of $\mu = 1.7549$ and highest inhibition efficiency (95%). The dipole moment is another indicator of the electronic distribution within a molecule. Some authors state that the inhibition efficiency increases with increasing values of the dipole moment, which depends on the type and nature of molecules considered. However, there is a lack of agreement in the literature on the correlation between μ and % IE, as in some cases no significant relationship between these values has been identified [70,71].

The number of electrons transferred (ΔN) was also calculated and tabulated in Table 5. Generally, value of ΔN shows inhibition efficiency resulting from electron donation, and the inhibition efficiency increases with the increase in electron-donating ability to the metal surface. Value of ΔN show inhibition effect resulted from electrons donation. According to Lukovits's study [72], if $\Delta N < 3.6$, the inhibition efficiency increases with increasing electron-donating ability at the metal surface. Based on these calculations, it is expected that the synthesized inhibitor is donor of electrons, and the steel surface is the acceptor, and this favors chemical adsorption of the inhibitor on the electrode surface. Here the inhibitor binds to the steel surface and forms an adsorption layer against corrosion.

Table 5. Calculated quantum chemical parameters of the studied compound

Quantum parameters	QIN3
E_{HOMO} (eV)	-8.7348
E_{LUMO} (eV)	-5.6871
ΔE_{gap} (eV)	3.0477
μ (debye)	1.7549
$I = -E_{HOMO}$	8.7348
$A = -E_{LUMO}$	5.6871
$\chi = \frac{I + A}{2}$	7.21095
$\eta = \frac{I - A}{2}$	1.52385
$\Delta N = \frac{\chi_{Fe} - \chi_{inh}}{2(\eta_{Fe} + \eta_{inh})}$	-0.0692161
TE (eV)	-16471.56505

The Mulliken charge distribution of QIN3 is presented in Table 6. It has been reported that as the Mulliken charges of the adsorbed center become more negative, the atom more easily donates its electron to the unoccupied orbital of the metal [73]. It could be readily observed that nitrogen, oxygen and some carbon atoms have high charge densities. The regions of highest electron density are generally the sites to which electrophiles can attach [74]. Therefore, N, O and some C atoms are the active centers, which have the strongest ability to bond to the metal surface. Conversely, some carbon atoms carry positive charges, which are often sites where nucleophiles can attach. Therefore, QIN3 can also accept electrons from Fe through these atoms. It has been reported that excellent corrosion inhibitors can not only offer electrons to unoccupied orbitals of the metal but also accept free electrons from the metal [75].

Table 6. Mulliken atomic charges of the QIN3 molecule

Atom	Charge	Atom	Charge	Atom	Charge
1 C	0.068258	8 C	0.027640	15 N	-0.556800
2 C	0.224342	9 H	0.194585	16 O	-0.569644
3 C	-0.004697	10 H	0.193968	17 H	0.359798
4 C	-0.145724	11 C	-0.193446	18 C	-0.502097
5 C	-0.229894	12 C	-0.218323	19 H	0.266775
6 H	0.218252	13 H	0.220274	20 H	0.266780
7 C	0.306030	14 H	0.191163	21 C	0.364798
22 N	0.482038				

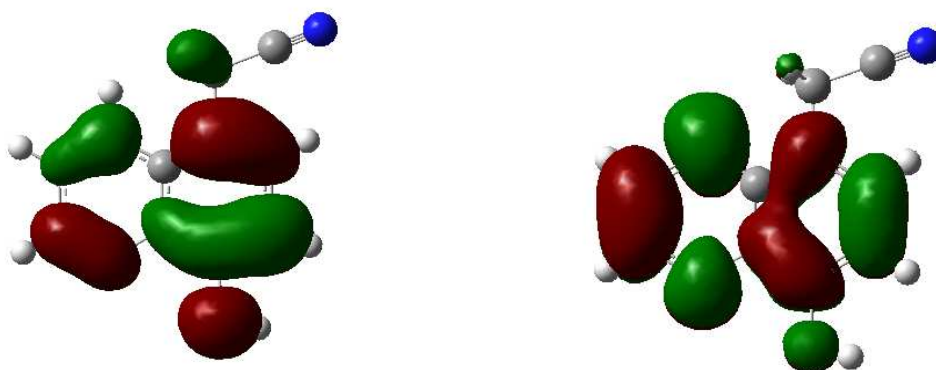


Figure 10. The HOMO (left) and LUMO (right) of QIN3

According to the description of frontier orbital theory, HOMO (Figure 10) is often associated with the electron donating ability of an inhibitor molecule. High E_{HOMO} values indicate that the molecule has a tendency to donate electrons to a metal with unoccupied molecule orbitals. E_{LUMO} , conversely, indicates the ability of the molecule to

accept electrons [76]. A lower value of E_{LUMO} indicates an easier acceptance of electrons from a metal surface [77]. The gap between the LUMO and HOMO energy levels of inhibitor molecules is another important parameter. Low absolute values of the energy band gap ($E = E_{LUMO} - E_{HOMO}$) mean good inhibition efficiency [78].

CONCLUSION

In this study, a new 2-(8-hydroxyquinoxalin-5-yl)acetonitrile (QIN3), was tested as corrosion inhibitor for carbon steel in 1.0 M HCl by using polarization and electrochemical impedance spectroscopy (EIS) at 303-333 K. The inhibition efficiency of QIN3 decreases in the temperature range 303-333 K. Changes in the electrochemical impedance spectroscopy (EIS) and potentiodynamic polarization were used to study the corrosion inhibition of carbon steel in 1.0 M HCl solutions at 303K using different concentrations of QIN3 as an inhibitor. This compound exhibited excellent inhibition performance as a mixed-type inhibitor. In general, the acidic corrosion of carbon steel was reduced upon the addition of an appropriate concentration of QIN3. The inhibition efficiencies obtained from the EIS data were comparable to those obtained from the polarization measurements in that they were greater for the inhibitory solution than those of the non-inhibitory solution. QIN3 acts as an efficient corrosion inhibitor in 1.0 M hydrochloric acid and it exhibits a maximum inhibition efficiency of 95%. The adsorption of QIN3 on a carbon steel surface obeys the Langmuir adsorption isotherm. The correlation between the quantum chemical parameters and inhibition efficiencies of QIN3 was investigated using DFT calculations. The inhibition efficiencies of the inhibitor are closely related to the quantum chemical parameters E_{HOMO} , E_{LUMO} and dipole moment. The fact that inhibition efficiency is increased with an increase in E_{HOMO} value and with a decrease in E_{LUMO} value has been established herein.

REFERENCES

- [1] G. Trabaneli, *Corrosion*, **1991**, 47, 410.
- [2] S. E. Nataraja, T. V. Venkatesha, K.Manjunatha, B. Poojary, M. K. Pavithra, and H. C. Tandon, *Corros. Sci.*, **2011**, 53, 2651.
- [3] U.J. Naik, V.A. Panchal, A.S. Patel, N.K. Shah, *J. Mater. Environ. Sci.*, **2012**, 3, 935.
- [4] A. Zarrouk, H. Zarrok, R. Salghi, B. Hammouti, F. Bentiss, R. Tourir, M. Bouachrine, *J. Mater. Environ. Sci.*, **2013**, 4, 177.
- [5] M. Yadav, S. Kumar, U. Sharma, P.N. Yadav, *J. Mater. Environ. Sci.*, **2013**, 4 (5), 691.
- [6] A. K. Singh, M. A. Quraishi, *J. Mater. Environ. Sci.*, **2010**, 1, 101.
- [7] U.J. Naik, V.A. Panchal, A.S. Patel, N.K. Shah, *J. Mater. Environ. Sci.*, **2012**, 3, 935.
- [8] H. Ashassi-Sorkhabi, Z. Ghasemi, D. Seifzadeh, *Appl. Surf. Sci.*, **2005**, 249, 408.
- [9] A. Samide, I. Bibicu, *Surf. Interf. Anal.*, **2008**, 40, 944.
- [10] U. Ergun, D. Yuzer, K.C. Emregul, *Mater. Chem. Phys.*, **2008**, 109, 492.
- [11] A. Zarrouk, B. Hammouti, H. Zarrok, R. Salghi, A. Dafali, Lh. Bazzi, L. Bammou, S. S. Al-Deyab, *Der Pharm. Chem.*, **2012**, 4, 337.
- [12] A. Zarrouk, B. Hammouti, H. Zarrok, S.S. Al-Deyab, M. Messali, *Int. J. Electrochem. Sci.*, **2011**, 6, 6261.
- [13] H. Zarrok, R. Saddik, H. Oudda, B. Hammouti, A. El Midaoui, A. Zarrouk, N. Benchat, M. Ebn Touhami, *Der Pharm. Chem.*, **2011**, 3, 272.
- [14] D. Ben Hmamou, R. Salghi, A. Zarrouk, B. Hammouti, S.S. Al-Deyab, Lh. Bazzi, H. Zarrok, A. Chakir, L. Bammou, *Int. J. Electrochem. Sci.*, **2012**, 7, 2361.
- [15] A. Zarrouk, B. Hammouti, A. Dafali, H. Zarrok, *Der Pharm. Chem.*, **2011**, 3, 266.
- [16] A. Ghazoui, R. Saddik, N. Benchat, B. Hammouti, M. Guenbour, A. Zarrouk, M. Ramdani, *Der Pharm. Chem.*, **2012**, 4, 352.
- [17] A. Zarrouk, B. Hammouti, H. Zarrok, I. Warad, M. Bouachrine, *Der Pharm. Chem.*, **2011**, 3, 263.
- [18] A.H. Al Hamzi, H. Zarrok, A. Zarrouk, R. Salghi, B. Hammouti, S.S. Al-Deyab, M. Bouachrine, A. Amine, F. Guenoun, *Int. J. Electrochem. Sci.*, **2013**, 8, 2586.
- [19] A. Ghazoui, N. Bencat, S.S. Al-Deyab, A. Zarrouk, B. Hammouti, M. Ramdani, M. Guenbour, *Int. J. Electrochem. Sci.*, **2013**, 8, 2272.
- [20] D. Ben Hmamou, R. Salghi, A. Zarrouk, M. Messali, H. Zarrok, M. Errami, B. Hammouti, Lh. Bazzi, A. Chakir, *Der Pharm. Chem.*, **2012**, 4, 1496.
- [21] A. Zarrouk, H. Zarrok, R. Salghi, N. Bouroumane, B. Hammouti, S.S. Al-Deyab, R. Touzani, *Int. J. Electrochem. Sci.*, **2012**, 7, 10215.
- [22] H. Bendaha, A. Zarrouk, A. Aouniti, B. Hammouti, S. El Kadiri, R. Salghi, R. Touzani, *Phys. Chem. News*, **2012**, 64, 95.
- [23] A. Zarrouk, B. Hammouti, H. Zarrok, M. Bouachrine, K.F. Khaled, S.S. Al-Deyab, *Int. J. Electrochem. Sci.*, **2012**, 6, 89.

- [24] S. Rekkab, H. Zarrok, R. Salghi, A. Zarrouk, Lh. Bazzi, B. Hammouti, Z. Kabouche, R. Touzani, M. Zougagh, *J. Mater. Environ. Sci.*, **2012**, 3, 613.
- [25] A. Ghazoui, R. Saddik, N. Benchat, M. Guenbour, B. Hammouti, S.S. Al-Deyab, A. Zarrouk, *Int. J. Electrochem. Sci.*, **2012**, 7, 7080.
- [26] H. Zarrok, A. Zarrouk, R. Salghi, Y. Ramli, B. Hammouti, M. Assouag, E. M. Essassi, H. Oudda and M. Taleb, *J. Chem. Pharm. Res.*, **2012**, 4, 5048.
- [27] H. Zarrok, K. Al Mamari, A. Zarrouk, R. Salghi, B. Hammouti, S. S. Al-Deyab, E. M. Essassi, F. Bentiss, H. Oudda, *Int. J. Electrochem. Sci.*, **2012**, 7, 10338.
- [28] J. Hmimou, A. Rochdi, R. Touir, M. Ebn Touhami, E.H. Rifi, A. El Hallaoui, A. Anouar, , D. Chebab, *J. Mater. Environ. Sci.*, **2012**, 3, 543.
- [29] M. Cenoui, N. Dkhireche, O. Kassou, M. Ebn Touhami, R. Touir, A. Dermaj, N. Hajjaji, *J. Mater. Environ. Sci.*, **2010**, 1, 84.
- [30] A. El Assyry, B. Benali, B. Lakhrissi, M. El Faydy, M. Ebn Touhami, R. Touir, M. Touil, *Res. Chem. Intermed.*, **2013**, DOI 10.1007/s11164-013-1445-0.
- [31] D. Ben Hmamou, R. Salghi, A. Zarrouk, H. Zarrok, B. Hammouti, S. S. Al-Deyab, A. El Assyry, N. Benchat, M. Bouachrine, *Int. J. Electrochem. Sci.*, **2013**, 8, 1526.
- [32] C. Fiaud, A. Harch, D. Mallouh, and M. Tzinmann, *Corros. Sci.*, **1993**, 35, 1437.
- [33] I.B. Obot, N.O. Obi-Egbedi, A.O. Eseola, *Ind. Eng. Chem. Res.*, **2011**, 50, 2098.
- [34] H. Zarrok, A. Zarrouk, B. Hammouti, R. Salghi, C. Jama, F. Bentiss, *Corros. Sci.*, **2012**, 64, 243.
- [35] A. D. Becke, *J. Chem. Phys.*, **1992**, 96, 9489.
- [36] A. D. Becke, *J. Chem. Phys.*, **1993**, 98, 1372.
- [37] C. Lee, W. Yang, R.G. Parr, *Phys. Rev. B*, **1988**, 37, 785.
- [38] M.J. Frisch, G.W. Trucks, H.B. Schlegel, G.E. Scuseria, M.A. Robb, J.R. Cheeseman, J.A. Montgomery Jr., T. Vreven, K.N. Kudin, J.C. Burant, J.M. Millam, S.S. Iyengar, J. Tomasi, V. Barone, B. Mennucci, M. Cossi, G. Scalmani, N. Rega, G.A. Petersson, H. Nakatsuji, M. Hada, M. Ehara, K. Toyota, R. Fukuda, J. Hasegawa, M. Ishida, T. Nakajima, Y. Honda, O. Kitao, H. Nakai, M. Klene, X. Li, J.E. Knox, H.P. Hratchian, J.B. Cross, C. Adamo, J. Jaramillo, R. Gomperts, R.E. Stratmann, O. Yazyev, A.J. Austin, R. Cammi, C. 870 H. Ju et al. / *Corrosion Science* 50 (2008) 865-871 Pomelli, J.W. Ochterski, P.Y. Ayala, K. Morokuma, G.A. Voth, P. Salvador, J.J. Dannenberg, V.G. Zakrzewski, S. Dapprich, A.D. Daniels, M.C. Strain, O. Farkas, D.K. Malick, A.D. Rabuck, K. Raghavachari, J.B. Foresman, J.V. Ortiz, Q. Cui, A.G. Baboul, S. Clifford, J. Cioslowski, B.B. Stefanov, G. Liu, A. Liashenko, P. Piskorz, I. Komaromi, R.L. Martin, D.J. Fox, T. Keith, M.A. Al- Laham, C.Y. Peng, A. Nanayakkara, M. Challacombe, P.M.W. Gill, B. Johnson, W. Chen, M.W. Wong, C. Gonzalez, J.A. Pople, Gaussian 03, Revision C.02, Gaussian Inc., Pittsburgh, PA, **2003**.
- [39] E.S. Ferreira, C. Giancomelli, F.C. Giacomelli, A. Spinelli, *Mater. Chem. Phys.*, **2004**, 83, 129.
- [40] M. Lebrini, M. Lagrenee, H. Vezin, M. Traisnel, F. Bentiss, *Corros. Sci.*, **2009**, 49, 2254.
- [41] P. Bommersbach, C. Alamany-Ddmont, J.P. Millet, B. Normand, *Electrochem. Acta*, **2006**, 51, 4011.
- [42] A.K. Singh, M.A. Quraishi, *Corros. Sci.*, **2009**, 51, 2752.
- [43] M.G. Hosseini, M. Ehteshamzadeh, T. Shahrabi, *Electrochim. Acta*, **2007**, 52, 3680.
- [44] F. Bentiss, M. Traisnel, M. Lagrenee, *Corros. Sci.*, **2000**, 42, 127.
- [45] Y. ELaoufir, H. Bourazmi, H. Serrar, H. Zarrok, A. Zarrouk, B. Hammouti, A. Guenbour, S. Boukhriss and H. Oudda, *Der Pharmacia Lettre*, **2014**, 6, 526.
- [46] A. Popova, E. Sokolova, S. Raicheva, and M. Christov, *Corros. Sci.*, **2003**, 45, 33.
- [47] X. Li and G. Mu, *Appl. Surf. Sci.*, **2005**, 252, 1254.
- [48] T. Szauer and A. Brandt, *Electrochimica Acta*, **1981**, 26, 1219.
- [49] S. S. Abd El Rehim, M. A. M. Ibrahim, and K. F. Khalid, *Mater. Chem. Phys.*, **2001**, 70, 268.
- [50] A. Zarrouk, B. Hammouti, A. Dafali, F. Bentiss, *Ind. Eng. Chem. Res.*, **2013**, 52, 2560.
- [51] B. Ateya, B.E. El-Anadouli, F.M. El-Nizamy, *Corros. Sci.* **1984**, 24, 509.
- [52] L.J. Vracar, D.M. Drazic, *Corros. Sci.*, **2002**, 44, 1669.
- [53] H. Keles, M. Keles, I. Dehri, O. Serindag, *Colloids Surf. A*, **2008**, 320, 138.
- [54] M. Abdallah, *Corros. Sci.*, **2002**, 44, 717.
- [55] T. Arslan, F. Kandemirli, E. Ebens, I. Love, H. Alemu, *Corros. Sci.*, **2009**, 51, 35.
- [56] N.O. Obi-Egbedi, *Corros. Sci.*, **2011**, 53, 263.
- [57] R.G. Parr, R.A. Donnelly, M. Levy, W.E. Palke, *J. Chem. Phys.*, **1978**, 68, 3801.
- [58] R.G. Parr, R.G. Pearson, *J. Am. Chem. Soc.*, **1983**, 105, 7512.
- [59] T. Koopmans, *Physica*, **1933**, 1, 104.
- [60] R.G. Pearson, *J. Am. Chem. Soc.*, **1963**, 85, 3533.
- [61] A. Lesar, I. Milosev *Chem.Phys.Lett.*, **2009**, 483, 198.
- [62] S. Martinez, *Mater. Chem. Phys.*, **2002**, 77, 97.
- [63] R.G. Pearson, *Inorg. Chem.*, **1988**, 27, 734.
- [64] V.S. Sastri, J.R. Perumareddi, *Corros. Sci.*, **1997**, 53, 617.

-
- [65] M.J.S. Dewar, W. Thiel *J. Am. Chem. Soc.*, **1977**, 99, 4899.
- [66] H.J. Chermette, *Comput Chem.*, **1997**, 20, 129.
- [67] F. Kandemirli, S. Sagdinc, *Corros. Sci.*, **2007**, 49, 2118.
- [68] A.A. Al-Amiery, A.Y. Musa, A.A.H. Kadhum, A. Mohamad, *Molecules*, **2011**, 16, 6833.
- [69] J.M. Costa, J.M. Lluch, *Corros. Sci.*, **1984**, 24, 924.
- [70] N. Khalil, *Electrochim. Acta*, **2003**, 48, 2635.
- [71] G. Bereket, C. Ogretir, A. Yurt, *J. Mol. Struct. (Theochem.)*, **2001**, 571, 139.
- [72] I. Lukovits, E. Kalman, F. Zucchi, *Corrosion*, **2001**, 57, 3.
- [73] S. Xia, M. Qiu, L. Yu, F. Liu, H. Zhao, *Corros. Sci.*, **2008**, 50, 2021.
- [74] A.Y. Musa, A.H. Kadhum, A.B. Mohamad, A.B. Rahoma, H. Mesmari, *J. Mol. Struct.*, **2010**, 969, 233.
- [75] I.B. Obot, E.E. Ebenso, I.A. Akpan, Z.M. Gasem, S. Afolabi Ayo, *Int. J. Electrochem. Sci.*, **2012**, 7, 1978.
- [76] I.B. Obot, N.O. Obi-Egbedi, *Curr. Appl. Phys.*, **2011**, 11, 382.
- [77] I.B. Obot, N.O. Obi-Egbedi, A.O. Eseola, *Ind. Eng. Chem. Res.*, **2011**, 50, 2098.
- [78] I.B. Obot, N.O. Obi-Egbedi, *Corros. Sci.*, **2010**, 52, 657.